

# Preparation and Characterization of Polyaluminum Titanium Silicate and its Performance in the Treatment of Low-Turbidity Water

## Authors:

Lina Liao, Peng Zhang

Date Submitted: 2018-08-28

Keywords: zeta potential, low turbidity, polyaluminum titanium silicate chloride, coagulant

## Abstract:

Using conventional coagulant, low turbidity water is difficult to achieve standard. This research uses aluminum chloride, titanium tetrachloride, and sodium silicate as raw materials for the preparation of polyaluminum titanium silicate chloride (PATC). PATC is used to treat low turbidity. The synthetic PATC showed the best coagulating effect in treated water under the following experimental conditions: Reaction temperature of 50 °C, and  $n(\text{Ti})/n(\text{Al})$ ,  $n(-\text{OH})/n(\text{Ti}+\text{Al})$ , and  $n(\text{Si})/n(\text{Ti}+\text{Al})$  were 0.3, 0.2, and 1.0, respectively. The species distribution and the transformation of PATC showed that the interaction between titanium tetrachloride, sodium silicate, and the hydrolysate of Al influenced the morphology distribution of Al. Temperature and -OH greatly affected the distribution of Al in PATC. The analysis of infrared spectra and X-ray diffraction indicated that both titanium tetrachloride and sodium silicate had complex chemical reactions with aluminum chloride. Si-O-Ti and Si-O-Al produced by the reaction affected the PATC treatment of low-turbidity water. Scanning electron microscopy showed, that compared with polyaluminum chloride(PAC), the PATC cluster was more compact, showed greater pore structure, and presented better flocculation precipitation. The optimal reaction conditions were an initial turbidity of 10 nephelometric turbidity unit(NTU), PATC dosage of 9 mg/L, pH of 8 for the simulated water sample, stirring speed of 50 r/min, and settling time of 50 min, which were determined by Orthogonal experiment. The zeta potential of the reaction process was analyzed. In the treatment of low-turbidity water, PATC mainly functioned by adsorbing, bridging, and sweeping flocculation. Electrical neutralization played an auxiliary role.

Record Type: Published Article

Submitted To: LAPSE (Living Archive for Process Systems Engineering)

Citation (overall record, always the latest version):

LAPSE:2018.0429

Citation (this specific file, latest version):

LAPSE:2018.0429-1

Citation (this specific file, this version):

LAPSE:2018.0429-1v1

DOI of Published Version: <https://doi.org/10.3390/pr6080125>

License: Creative Commons Attribution 4.0 International (CC BY 4.0)

Article

# Preparation and Characterization of Polyaluminum Titanium Silicate and its Performance in the Treatment of Low-Turbidity Water

Lina Liao and Peng Zhang \* 

School of Civil Engineering, Hunan University of Science and Technology, Xiangtan 411201, China; liaolina523@163.com

\* Correspondence: zhangpeng388@126.com or 1020126@hnust.edu.cn; Tel.: +86-0731-58290251

Received: 17 July 2018; Accepted: 8 August 2018; Published: 11 August 2018



**Abstract:** Using conventional coagulant, low turbidity water is difficult to achieve standard. This research uses aluminum chloride, titanium tetrachloride, and sodium silicate as raw materials for the preparation of polyaluminum titanium silicate chloride (PATC). PATC is used to treat low turbidity. The synthetic PATC showed the best coagulating effect in treated water under the following experimental conditions: Reaction temperature of 50 °C, and  $n(\text{Ti})/n(\text{Al})$ ,  $n(-\text{OH})/n(\text{Ti}+\text{Al})$ , and  $n(\text{Si})/n(\text{Ti}+\text{Al})$  were 0.3, 0.2, and 1.0, respectively. The species distribution and the transformation of PATC showed that the interaction between titanium tetrachloride, sodium silicate, and the hydrolysate of Al influenced the morphology distribution of Al. Temperature and -OH greatly affected the distribution of Al in PATC. The analysis of infrared spectra and X-ray diffraction indicated that both titanium tetrachloride and sodium silicate had complex chemical reactions with aluminum chloride. Si-O-Ti and Si-O-Al produced by the reaction affected the PATC treatment of low-turbidity water. Scanning electron microscopy showed, that compared with polyaluminum chloride(PAC), the PATC cluster was more compact, showed greater pore structure, and presented better flocculation precipitation. The optimal reaction conditions were an initial turbidity of 10 nephelometric turbidity unit(NTU), PATC dosage of 9 mg/L, pH of 8 for the simulated water sample, stirring speed of 50 r/min, and settling time of 50 min, which were determined by Orthogonal experiment. The zeta potential of the reaction process was analyzed. In the treatment of low-turbidity water, PATC mainly functioned by adsorbing, bridging, and sweeping flocculation. Electrical neutralization played an auxiliary role.

**Keywords:** coagulant; polyaluminum titanium silicate chloride; low turbidity; zeta potential

## 1. Introduction

With the rapid development of the social economy, water pollution and water scarcity are becoming increasingly serious. However, people's demand for water quality is increasing. Additionally, the sustainable development of water resources has attracted increasing attention from scholars [1,2]. In several studies on drinking water quality requirements, stringent requirements for the turbidity of water quality have been proposed. The low turbidity of water refers to the turbidity of the original water of rivers or lakes that is less than 30 NTU [3]. The concentration of suspended particles in low-turbidity water is relatively low, and the particle size is small and evenly distributed in the water. Impurities in water usually exist in the form of colloids and thus have good dynamic and aggregation stability. When the turbidity of water is low, the probabilities of a collision between particles, occurrence of a reaction, and formation of flocculation are low, thus, water cannot settle easily [4,5]. At present, the treatment of low-turbidity water mainly includes chemical medicine optimization, enhanced

coagulation, sludge recycling technology, dissolved air flotation, micro flocculation contacting filter technology, pre-oxidation technology, and advanced treatment [6,7].

Coagulation–precipitation is one of the important steps in the treatment of drinking water. After conventional treatment, such as coagulation and precipitation filtration, water can reach the turbidity standard of drinking water. Therefore, the selection of effective coagulants is one of the key steps in drinking water treatment. The main coagulant used in China is aluminum coagulant. However, the use of a single aluminum coagulant has corresponding drawbacks, for example, the residual aluminum residue caused using an aluminum coagulant is harmful to the human nervous system [8,9]. Polysilicic acid is a cheap and harmless inorganic polymer coagulant that is stable and durable. It is effective in water turbidity treatment after polymerization of aluminum salt or iron salt coagulant. The introduction of polysilicic acid increases the flocculant molecular weight, and studies have reported that the combination of polysilicic acid and metal salts can improve the ability of adsorption and net capture to ultimately improve the flocculation capacity of flocculants [10–13]. In addition, polysilicic acid can reduce the content of residual aluminum when combined with aluminum salt coagulant [13,14]. Titanium is an abundant element that is widely distributed in the lithosphere and crust, and its reserves are the ninth most abundant among the reserves of all elements [15,16]. Titanium is non-toxic and does not react with the human body, so, it is also widely used in medical treatment [17]. Furthermore, titanium salt coagulants exert good treatment effects on turbidity, chromaticity, and so on. As a coagulant, titanium salt can be used to recycle sludge and produce valuable  $\text{TiO}_2$  for reuse [18–20]. An increasing number of scholars use titanium salt as a coagulant for water treatment. Chekli et al. [21] studied the coagulation effect and coagulation mechanism of polymerized titanium salt, and found that it had better treatment effect on algal turbid water. Chang et al. [3] prepared a polyaluminum titanium silicate sulfate coagulant by copolymerization and investigated the effects of treatment with turbid water, and the residual turbidity was 0.36 NTU after treatment.

In the present study, we present the preparation process of polyaluminum titanium silicate chloride (PATC). PATC was prepared by sodium silicate, aluminum chloride, and titanium tetrachloride, and this study presents for the first time the preparation process of polyaluminum titanium silicate chloride and its flocculation performance to low turbid water, therefore, this study is of importance to the treatment of low turbid water. The low-turbidity water was from a school lake. In this study, different molar ratios of Ti to Al ( $n(\text{Ti})/n(\text{Al})$ ),  $n(-\text{OH})/n(\text{Ti}+\text{Al})$ , and  $n(\text{Si})/n(\text{Ti}+\text{Al})$  and different reaction temperatures were considered and analyzed to determine the effects of coagulant treatment on low-turbidity water. The species distribution and the transformation of PATC were investigated by the Al-Ferron complex timed colorimetric method. The structures and morphologies of PATC were characterized by Fourier transform infrared spectroscopy (FTIR), X-ray diffraction (XRD), and scanning electron microscope-energy dispersive spectrum (SEM-EDS). The optimum hydraulic conditions and the reaction mechanisms of PATC in treating low-turbidity water were determined by orthogonal test design and zeta potential monitoring analysis.

## 2. Materials and Methods

### 2.1. Materials

All reagents used were of analytical reagent grade, except  $\text{TiCl}_4$ , which was chemically pure. Aluminium chloride ( $\text{AlCl}_3$ ) was obtained from Tianjin hengxing chemical reagent company (Tianjin, China). Sodium hydroxide (NaOH) was purchased from Xilong Scientific Co., Ltd. (Shantou, China). Sodium silicate ( $\text{Na}_2\text{SiO}_3$ ) was supplied by Hunan Huihong Reagent Co., Ltd. (Changsha, China). Titanium tetrachloride ( $\text{TiCl}_4$ ) was produced by Damao Chemical Reagent Industrial company (Tianjin, China). Concentrated sulfuric acid ( $\text{H}_2\text{SO}_4$ ) was obtained from Zhuzhou Starry Glass Co., Ltd. (Zhuzhou, China). All aqueous solutions and standard solutions were prepared with de-ionized water. The electronic analytical balance that was used to weigh drugs was obtained from Shanghai Hengping Scientific Instrument Co., Ltd. (Shanghai, China). The PB-10 acidity meter was bought from Sartorius

Scientific Instrument (Beijing, China) Co., Ltd. (Beijing, China). The ZR4-6 mixer was purchased from ZhongRun Water Industry Technology Development Co., Ltd. (Shenzhen, China). The heat-collecting magnetic stirrer was supplied by Bonsai Instrument Technology (Shanghai, China) Co., Ltd. (Shanghai, China). The 2100Q turbidimeter was produced by HACH (Loveland, USA). The Nicolet6700 FTIR was sourced from Thermo Fisher Scientific Company (Waltham, USA). The JSM-6380LV SEM was obtained from JEOL (Tokyo, Japan). The ultraviolet-visible spectrophotometer (twin-beam type tu-1901) was produced by Beijing Purkinje General Instrument (Beijing, China). Co., Ltd. And the 8D-Advance XRD was purchased from Germany (Karlsruhe, Germany). The zetasizer 2000 was obtained from Malvern (Malvern, UK).

## 2.2. Synthesis of PATC

(1) Configured 0.5 mol/L of sodium silicate solution. The pH of the solution was adjusted with concentrated sulfuric acid until its pH was less than 3. The polysodium silicate solution was obtained by magnetic stirring for 1 h at room temperature.

(2) A certain quality of  $\text{AlCl}_3$  was dissolved into a deionized water solution and then frozen for 30 min until crystals appeared.  $\text{TiCl}_4$  was added to the  $\text{AlCl}_3$  solution with crystals. Subsequently, NaOH was completely dissolved in the mixed aqueous solution under continuous stirring at room temperature. Stirring was continued in the water bath for 1 h.

(3) The products obtained from steps (1) and (2) were mixed with magnetic force for 1 h under certain conditions. Finally, PATC was obtained by curing for 24 h.

## 2.3. Coagulation Experiment

The simulated water samples were obtained from a lake in the Hunan University of Science and Technology. The turbidity range of the simulated water was 7–21 NTU, and the  $\text{pH} = 7.8 \pm 0.2$ . A certain dosage of PATC was immediately added to the simulated water samples. The mixture solution was first stirred at a high speed of 210 r/min for 2 min and then mixed at a low speed of 50 r/min for 10 min. After the static reaction was completed, the supernatant 2 cm away from the liquid surface was obtained, and the remaining water turbidity was determined by turbidimetry analysis.

## 2.4. The Morphological Analysis of Al

The species distribution and the transformation of PATC were investigated by the Al–Ferron complex timed colorimetric method. The reaction time with the ferron reagent between 0 and 1 min was defined as Ala, the reaction time with the ferron reagent between 1 and 120 min was defined as Alb, and the species that could not react with ferron in a limited time was defined as Alc [22], and the sum of the three equated to the total amount of aluminum. In this study, a morphological analysis of the object was carried out under the following reaction conditions for the preparation of PATC: Reaction temperatures of 30 °C, 40 °C, 50 °C, 60 °C, 70 °C, and 80 °C;  $n(\text{Ti})/n(\text{Al})$  was from 0.1 to 0.6;  $n(\text{Si})/n(\text{Al}+\text{Ti})$  was from 0.2 to 1.2; and  $n(-\text{OH})/n(\text{Al}+\text{Ti})$  was from 0.1 to 0.6.

The standard solution for the Al–Ferron reaction was configured with a standard curve of absorbance and concentration. The concentration of Al was  $0\text{--}8 \times 10^{-5}$  mol/L. The absorbance value of the Al–Ferron solution was determined at a 362 nm wavelength, with the absorbance (A) as the vertical coordinate and the concentration of Al as the horizontal coordinate. The standard curve was drawn and is shown in Figure 1. The regression equation was calculated as  $Y = 0.00947 + 0.08558X$ .

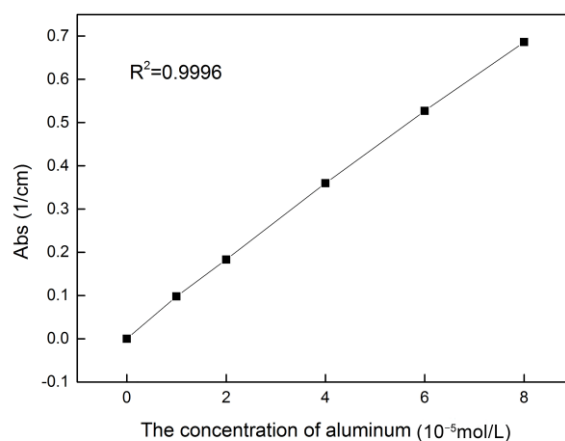


**Figure 1.** Ferron colorimetric determination of the aluminum standard curve.

### 2.5. Characterization of PATC

In this section, the physical and chemical structures of PATC were compared and analyzed. The liquid PATC was put into the 80 °C drum wind drying oven, and then dried and grinded into a powder. The powder samples were scanned by infrared spectroscopy, with a resolution of  $2\text{ cm}^{-1}$  and a range of  $400\text{--}4000\text{ cm}^{-1}$  wave number, and the method used in this experiment was the KBr pressure plate method. The specific characteristics of the samples were obtained from D8 ADVANCE XRD and then scanned and analyzed with Jade 6 software (Livermore, USA). The scanning angle control was  $5^{\circ}\text{--}90^{\circ}$ . The morphologies of PATC were obtained by scanning electron microscopy (SEM, Tokyo, Japan), and the specific element analysis of PATC was carried out via energy spectrum analysis (EDS, Tokyo, Japan).

### 2.6. Analysis of Flocculation Properties

To determine the optimal reaction conditions of flocculant PATC in the treatment of low-turbidity water and the mechanism of PATC in the treatment of low-turbidity water, this study adopted an orthogonal experiment design and analysis, and then performed a monitoring and analysis of the zeta potential. To explore the best conditions for PATC treatment of water with low turbidity, an orthogonal test of five factors and five levels ( $L_{25}(5^5)$ ) was designed. According to the preliminary analysis of the test and reference, the initial turbidity of water, the dosage of PATC, pH, stirring intensity, and precipitation time were the five factors in the orthogonal experiment. The water turbidity removal rate after the reaction was used as the evaluation index, and the specific contents of the orthogonal test on low-turbidity water in PATC are shown in Table 1.

**Table 1.**  $L_{25}(5^5)$  orthogonal experimental design table of polyaluminum titanium silicate chloride (PATC) as flocculants.

Levels	A	B	C	D	E
	Initial Turbidity (NTU)	PATC Dosage (mg/L)	pH	Stirring Intensity (r/min)	Precipitation Time (min)
1	5	1.8	5	30	10
2	10	3.6	6	50	20
3	15	5.4	7	70	30
4	20	7.2	8	90	40
5	25	9.0	9	110	50

The optimum water condition for PATC treatment of low-turbidity water was determined by orthogonal test data analysis. A zetasizer potentiometer was used to monitor the potential of the

flocculant PATC, simulated water sample, and flocculation process. By combining the flocculant, simulated water sample, and zeta potential of the reaction process, the reaction mechanism of PATC and low-turbidity water was studied.

### 3. Results and Discussion

#### 3.1. Effects of Different Preparation Conditions on Al Morphology and the Treatment of Low-Turbidity Water with PATC

##### 3.1.1. Effect of Different Reaction Temperatures on PATC Treatment of Low-Turbidity Water

Temperature exerts a great influence on the preparation of high-efficiency flocculant. Temperature can affect the hydrolysis of metal salts, and extremely high or excessively low temperatures are not conducive to the preparation of efficient coagulants [3,23]. To determine the optimum reaction temperature of PATC coagulant, six experiments were performed at different temperatures. Figure 2 shows that the treatment effect of PATC on low-turbidity water was decreased first and then leveled off when the dosage was greater than 10.8 mg/L. The best effect was observed when the reaction temperatures were 50 °C and 60 °C. However, considering the energy consumption and economic problem, it can be identified that the best reaction temperature was 50 °C. When the dosage of the coagulant was 10.8 mg/L, the remaining turbidity decreased to 0.48 NTU. The distribution of Al morphology in different reaction temperatures (as shown in Figure 3) indicated that different reaction temperatures have a certain influence on the shape of Al in PATC. Among them, the content of Ala was relatively high, and the main distribution was between 73.25% and 88.26%. However, the content of Alb and Alc was not very high. The Ala content of PATC when the reaction temperatures were 50 °C and 60 °C was higher than that when the reaction temperatures were 30 °C and 40 °C. The Alc content was high when the reaction temperatures were 70 °C and 80 °C because the reaction of Al (III) hydrolysis was an endothermic reaction [24]; the increase of temperature in a certain range was conducive to the increase of mass transfer and hydrolysis reaction. Thus, the content of Ala is increased by the formation of mononuclear hydroxyl ligand ions through complexation. In addition, it was found that when the reaction temperature was 50 °C, the content of Alc plummeted, possibly because of the introduction of Ti in PATC. The hydrolysis of Ti was also an endothermic process, and its ability to compete with hydroxyl was greater than that of Al. Therefore, under certain temperature conditions, Ti rapidly combined with the hydroxyl group to form a high-poly-degree titanium complex, which caused the formation of Alc to plummet. Thus, the treatment process of low-turbidity water was mainly handled by the synergistic action of Ti and Al.

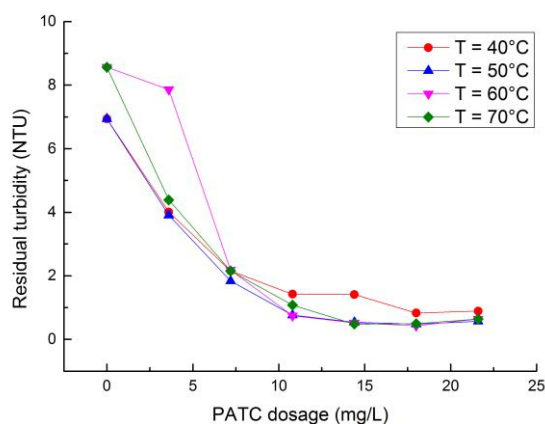
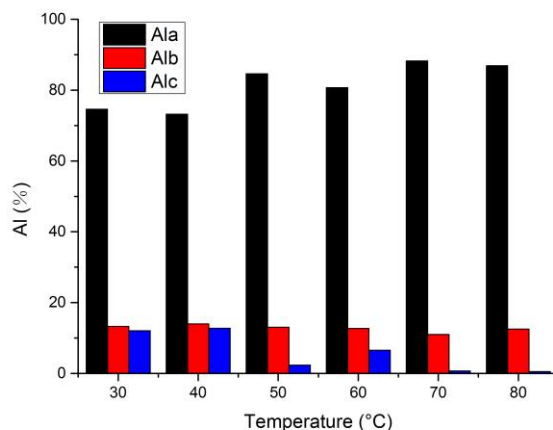


Figure 2. Effect of the temperature on the residual turbidity.



**Figure 3.** Effect of the temperature on the morphology of Al.

### 3.1.2. Effect of Different $n(\text{Ti})/n(\text{Al})$ on PATC Treatment of Low-Turbidity Water

In the reaction, the polymer produced by polymerization will have different effects on the treatment of low-turbidity water due to the different proportions of raw materials [20]. The main reaction materials of PATC in this study were  $\text{Na}_2\text{SiO}_3$ ,  $\text{TiCl}_4$ , and  $\text{AlCl}_3$ . Further experiments were conducted to further determine the optimum titanium–aluminum ratio of the prepared PATC coagulant for low-turbidity water treatment after determining the optimum reaction temperature at 50 °C. The experiment was fixed at a reaction temperature of 50 °C. The effect of different  $n(\text{Ti})/n(\text{Al})$  on the preparation of the PATC treatment of low-turbidity water is shown in Figure 4. The turbidity decreased with the addition of the coagulant, and the treatment effect was stable when the dosage was 10.8 mg/L. After treatment, the turbidity was reduced to 0.44 NTU. The effect of the coagulant prepared by  $n(\text{Ti})/n(\text{Al}) = 0.3$  and 0.4 was similar to the treatment effect of low-turbidity water, and the effect of  $n(\text{Ti})/n(\text{Al}) = 0.5$  and 0.6 was slightly better than that of the previous two. However, it can be determined that  $n(\text{Ti})/n(\text{Al}) = 0.3$  was the best ratio condition for the preparation of the coagulant in consideration of its treatment effect on low-turbidity water and economic benefits. Figure 5 presents the analysis of the distribution of Al morphology of PATC prepared under the ratio of  $n(\text{Ti})/n(\text{Al}) = 0.1$ –0.6. The graph indicates that Ala presented a roughly increasing process, whereas Alb and Alc presented a basic descending process, and Ala had a large proportion. The Ala content was between 60% and 85%, and reached the highest level when  $n(\text{Ti})/n(\text{Al})$  was 0.6. Alb and Alc showed a decreasing trend. Alc had the smallest proportion (15.06%–4.4%), and the Alb content range was 23.8%–10.59%. This phenomenon can be explained that the hydrolysis capacity of Ti is greater than that of Al, and as the  $n(\text{Ti})/n(\text{Al})$  ratio increases, the competitive ability of Al to -OH decreases, which makes the content of Alb and Alc decrease. Compared with Al (III), Ti (IV) had a stronger ability to compete with -OH. Furthermore, the hydrolysis forms of Ti (IV) were more inclined to form a high degree of polymerization of titanium complexes. The hydrolysis of the Al (III) form mainly resulted in mononuclear hydroxyl aluminum complexes. Therefore, the form of Al was mainly  $\text{Al}(\text{H}_2\text{O})_6^{3+}$ ,  $\text{Al}(\text{OH})(\text{H}_2\text{O})_5^{2+}$ , and other monomers and primers; obviously, there are more in the form of Ala. The PATC prepared with  $n(\text{Ti})/n(\text{Al}) = 0.3$  was the best treatment for low-turbidity water as it adsorbed the bridging bridge produced by the interaction between the bonds of Si-Al and Si-Ti [25], which were formed by the addition of polysilicic acid with Al salt and Ti salt.

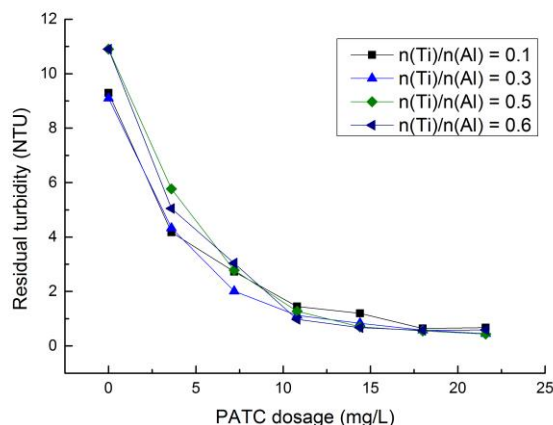


Figure 4. Effect of  $n(\text{Ti})/n(\text{Al})$  on the residual turbidity.

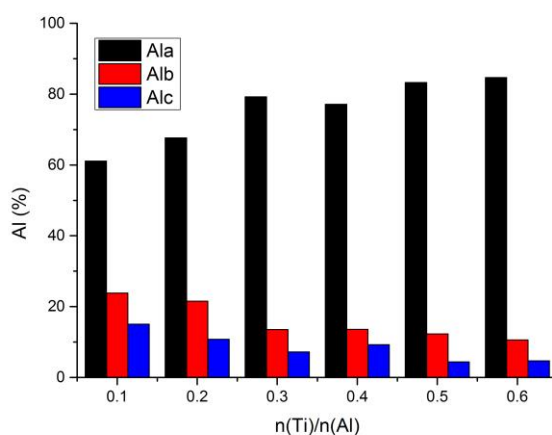


Figure 5. Effect of  $n(\text{Ti})/n(\text{Al})$  on the morphology of Al.

### 3.1.3. Effect of Different $n(\text{-OH})/n(\text{Al+Ti})$ on PATC Treatment of Low-Turbidity Water

In the present study, the effect of the flocculant was related to the hydrolysis degree of Ti and Al and the polymerization products. The proportion of NaOH added in the preparation of flocculant directly affected the hydrolysis of metal salt and the products synthesized by the flocculant [26,27]. To study the effect of  $n(\text{-OH})/n(\text{Al+Ti})$  on the treatment of low-turbidity water, we changed  $n(\text{-OH})/n(\text{Al+Ti}) = 0.1\text{--}0.6$  to determine the best PATC preparation of  $n(\text{-OH})/n(\text{Al+Ti})$  under a fixed optimal temperature and optimal  $n(\text{Ti})/n(\text{Al})$ . The treatment effect of different  $n(\text{-OH})/n(\text{Al+Ti})$  on low-turbidity water is shown in Figure 6. The figure indicates that the turbidity of water after the initial injection of PATC fell rapidly and became stable when the dosage was 10.8 mg/L. Moreover, PATC prepared with  $n(\text{-OH})/n(\text{Al+Ti}) = 0.2$  showed the best treatment effect on low-turbidity water, with the lowest turbidity being 0.44 NTU.

Figure 7 is an analysis of the morphology of Al in PATC. The figure shows that Ala occupied a larger proportion of the entire form of Al, and the content of Ala remained stable, with its content exceeding 80%. Ala had the largest content when  $n(\text{-OH})/n(\text{Al+Ti}) = 0.2$ ; the content of Ala reached 85.01%, whereas the content of Alc was the lowest at 1.29%. Alb increased with the increase of  $n(\text{-OH})/n(\text{Al+Ti})$  because as the ratio of -OH increased, the mononuclear hydroxyl complex further polymerized to form a polynuclear hydroxyl polymer, such as Al<sub>13</sub>. However, at  $n(\text{-OH})/n(\text{Al+Ti}) = 0.2$ , the content of Alc was the lowest, which may be explained by the effect of Ti hydrolysis; that is, as -OH increased, the hydroxyl polymer of Ti also increased. At the same time, the hydroxyl group was completed by the hydrolysis of Ti, which was supposed to react with Alb to form Alc. The increase



in hydroxyl polymer after hydrolysis enhanced the adsorption of the bridging bridge and sweep flocculation of the coagulant.

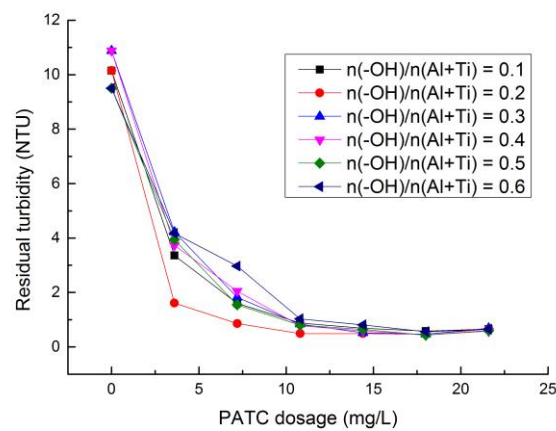


Figure 6. Effect of  $n(-OH)/n(Ti+Al)$  on the residual turbidity.

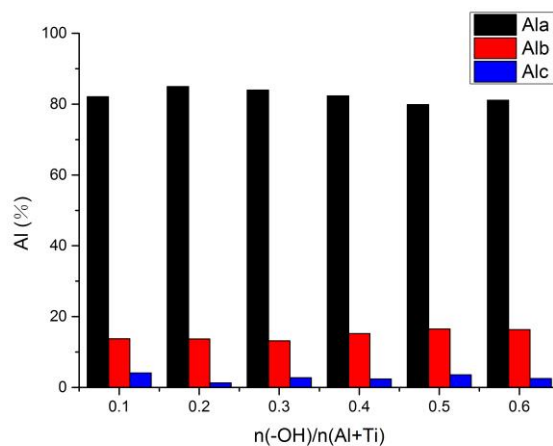


Figure 7. Effect of  $n(-OH)/n(Ti+Al)$  on the morphology of Al.

In water treatment, the low polymer hydrolysis products represented by Ala are mainly used for its charge neutralization capability. The component of Alb mainly addresses the treatment of pollutants, such as colloid, by adsorbing the bridging bridge and absorbing the neutralization ability to realize the purification of the water body. The high-polymer hydrolytic Al mainly flocculates the colloidal particles in the water by adsorbing the bridging bridge and sweep flocculation [28]. In combination with the morphological distribution of Al,  $n(-OH)/n(Al+Ti) = 0.2$  showed the best treatment effect on low-turbidity water because of the combined effect of the absorbed neutralization by Ala and the sweep flocculation by the hydroxyl polymer of Ti.

#### 3.1.4. Effect of Different $n(Si)/n(Ti+Al)$ on PATC Treatment of Low-Turbidity Water

Based on previous studies, the optimum temperature,  $n(Ti)/n(Al)$ , and  $n(-OH)/n(Ti+Al)$  of flocculant synthesis was determined. In this section, the effect of the reaction material, Si, on the synthesis and treatment of the flocculant was determined based on previous results [18,27]. Further study was conducted to ensure the optimum effect of  $n(Si)/n(Ti+Al)$  on the PATC treatment of low-turbidity water. The temperature was fixed at 50 °C,  $n(Ti)/n(Al) = 0.3$ , and  $n(-OH)/n(Al+Ti) = 0.2$ . We changed  $n(Si)/n(Ti+Al)$  in the preparation of the coagulant to determine the ratio with the best treatment effect on low-turbidity water. Figure 8 shows the PATC treatment of low-turbidity water with different  $n(Si)/n(Ti+Al)$ . The figure indicates that PATC exerted a good effect on low-turbidity water.

The turbidity of water decreased with the increase of PATC dosage, and a significant drop occurred when the dosage was 3.6 mg/L. It can be determined that  $n(\text{Si})/n(\text{Ti}+\text{Al}) = 1.0$  was the best treatment condition, which reached a stable state when the input volume reached 10.8 mg/L. The minimum turbidity decreased to 0.51 NTU, as shown in Figure 8. According to Figure 9, we analyzed the morphology of PATC under different  $n(\text{Si})/n(\text{Ti}+\text{Al})$  to realize the basic reaction mechanism of PATC treatment of low-turbidity water. Figure 9 indicates that, regardless of the percentage of preparation conditions, Ala had the highest levels and remained relatively stable. The content of Al was up to 80.73%, which indicated that the morphology of Al in the PATC was mainly in the form of mononuclear hydroxyl compounds, a few of which existed in the form of complex polymers. A comparison of the morphological distribution of Al under the PATC prepared with different ratios indicated that the content of Alc was the highest at 5.94% when  $n(\text{Si})/n(\text{Ti}+\text{Al}) = 1.0$ ; its value was 1.00% when  $n(\text{Si})/n(\text{Ti}+\text{Al}) = 0.2$ . This result may be closely related to the introduction of Si. It was indicated that the complex, Al-Si, aggregates its form between polysilicic acid and aluminum ions according to some literature [11,18]; such formation plays a role in adsorbing the bridging bridge. Furthermore, the polymer polysilicic acid polymerization forms a network structure; thus, sweep flocculation helps improve the flocculant ability and aids the treatment of low-turbidity water. In addition, the copolymerization of Ti and Si enhances the stability of coagulants in water, and the formation of large particles can help the removal of colloidal particles [29]. The treatment effect of PATC prepared by  $n(\text{Si})/n(\text{Ti}+\text{Al}) = 1.2$  was slightly lower than that of PATC prepared by  $n(\text{Si})/n(\text{Ti}+\text{Al}) = 1.0$ . These results are explained by the polysilicic acid being an anionic inorganic polymer flocculant. The high concentration of polysilicic acid reduces its power neutralization and flocculation capacity [29,30].

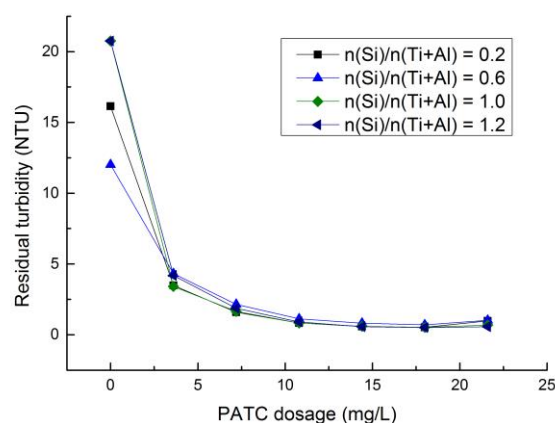


Figure 8. Effect of  $n(\text{Si})/n(\text{Ti}+\text{Al})$  on the residual turbidity.

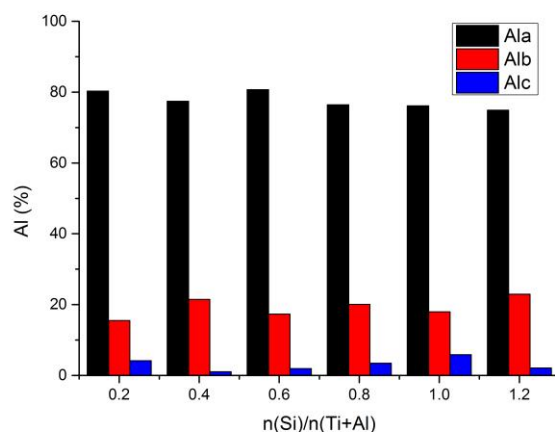


Figure 9. Effect of  $n(\text{Si})/n(\text{Ti}+\text{Al})$  on the morphology of Al.

### 3.2. Characterization

#### 3.2.1. Fourier Transform Infrared Spectroscopy

Figure 10 is a comparison of the infrared spectra of PAC and PATC prepared under different reaction conditions with the potassium bromide method. Table 2 presents the single variable of PATC (1–4) scale. The figure indicates a wide strong absorption peak at 3300–3500  $\text{cm}^{-1}$ , which was caused by the stretching vibration of -OH and the water molecules in the sample with Ti and Al [31]. The wave crest was wide, and a shoulder peak appeared, thereby suggesting that -OH existed in a different chemical environment. In addition, the comparison between the two spectra showed that PATC had a redshift at the peak point, and its absorption area was large; thus, more hydroxyl groups should form. A peak in the wave number of 1653.08  $\text{cm}^{-1}$  was observed because of the bending vibration of -OH in the PATC binding water. Figure 10 also shows a strong adsorption peak at 1560.36  $\text{cm}^{-1}$  that was not observed in the infrared spectrum of PAC. A potential explanation for this result is the stretching vibration of Si-O-Si in PATC. Furthermore, the peaks observed at roughly 1384.28  $\text{cm}^{-1}$  were attributed to the vibration adsorption bands of Al-O-Al and Si-O-Si [32], adsorption peak at 1094.67  $\text{cm}^{-1}$  was derived from the characteristic stretching vibration of associating Ti-O-Si and Si-O-Al [29], and a blue shift occurred in the PATC compared relative to the PAC. The peaks at 789.07 and 604.53  $\text{cm}^{-1}$  were sourced from characteristic groups of the stretching vibration of Ti-O-Ti, which was from the tetravalent complex produced by Ti ion hydrolysis [33].

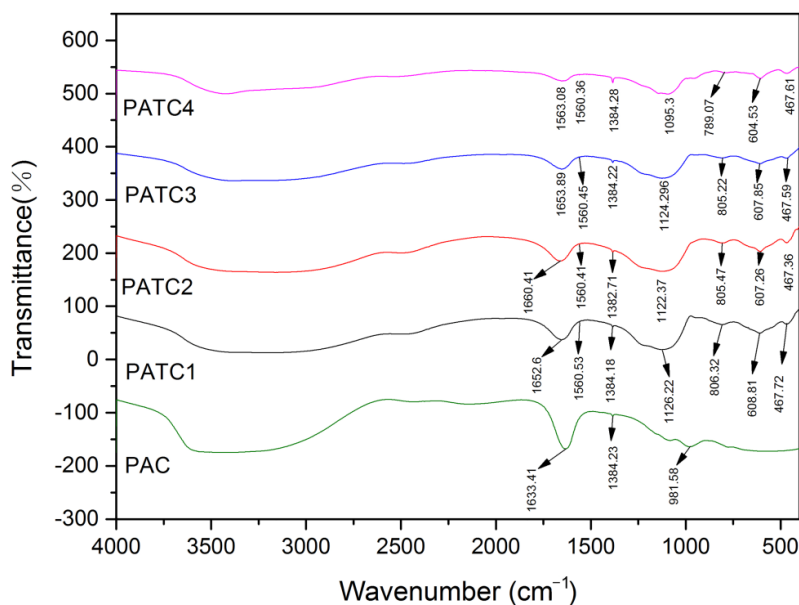


Figure 10. FTIR spectra of various samples.

Table 2. The single variable of PATC (1–4) scale.

Coagulant	Reaction Temperature (°C)	n(Ti)/n(Al)	n(-OH)/n(Ti+Al)	n(Si)/n(Ti+Al)
PATC 1	50	0.3	0.3	0.4
PATC 2	50	0.5	0.3	0.4
PATC 3	50	0.3	0.2	0.4
PATC 4	50	0.3	0.2	1

A new vibration peak was observed at 467.61  $\text{cm}^{-1}$ , which was attributed to the stretching vibration of Ti-O. This result also indicated that Ti in the prepared coagulant was not present in a single ionic form. The polymerization of aluminum chloride, titanium tetrachloride, and sodium silicate was not simply a physical function, but rather a complex chemical reaction.

### 3.2.2. X-Ray Diffraction Spectrogram Analysis

Figures 11 and 12 show the XRD patterns of PATC and polyaluminum chloride (PAC). The crystal material generated a diffraction peak at the angle determined on the diffraction pattern, whereas the non-crystalline material did not generate a diffraction peak, but rather a diffused peak packet [19]. By comparing the XRD spectra of PAC and PATC, it can be determined that the PATC peak intensity was much better than that of PAC. Figure 11 shows PATC inside without  $\text{TiCl}_4$  and a diffraction peak of  $\text{Na}_2\text{SiO}_3$ . Thus, it can be determined that the introduction of titanium and silicon produces new substances. By using Jade 6 to analyze the obtained XRD, it can be identified that new diffraction structures, such as  $\text{Na}_{1.75}\text{Al}_{1.75}\text{Si}_{0.25}\text{O}_4$ ,  $\text{Na}_{1.65}\text{Al}_{1.65}\text{Si}_{0.35}\text{O}_4$ ,  $\text{Na}_2\text{TiOSiO}_4$ , and  $\text{Al}_2\text{Si}_2\text{O}_5(\text{OH})_4$ , are present in PATC. Thus, we infer that aluminum chloride, sodium silicate, and titanium tetrachloride are more abundant than those occurring between materials, such as the mixture. However, a complex chemical reaction occurred, and a new type of inorganic macromolecule flocculation reagent was formed.

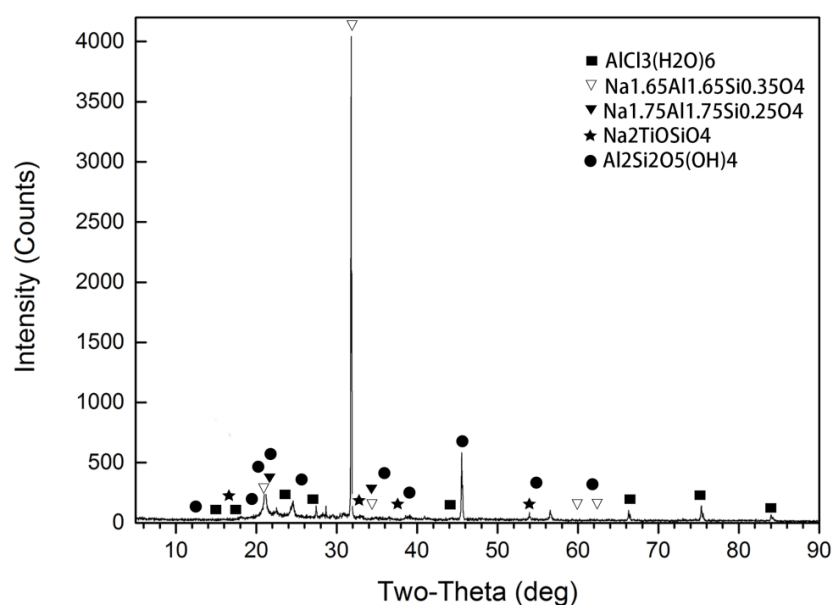


Figure 11. The XRD pattern of PATC.

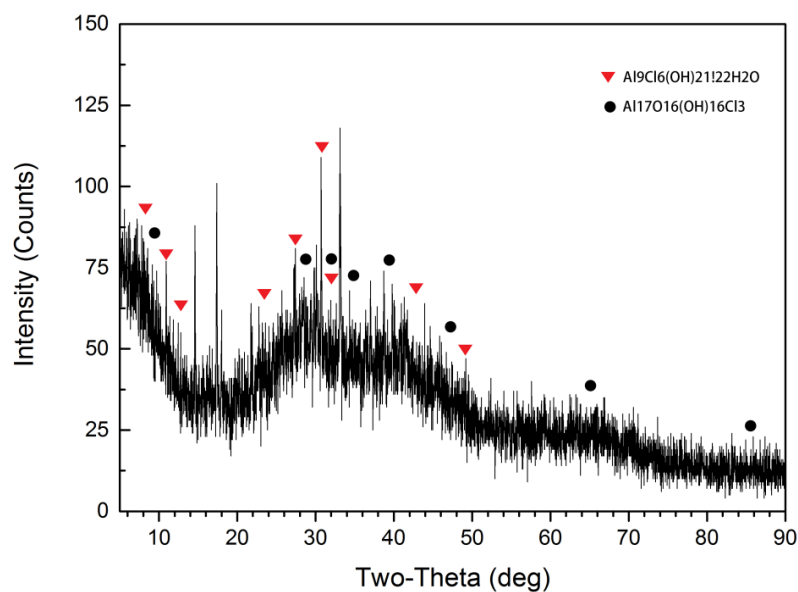
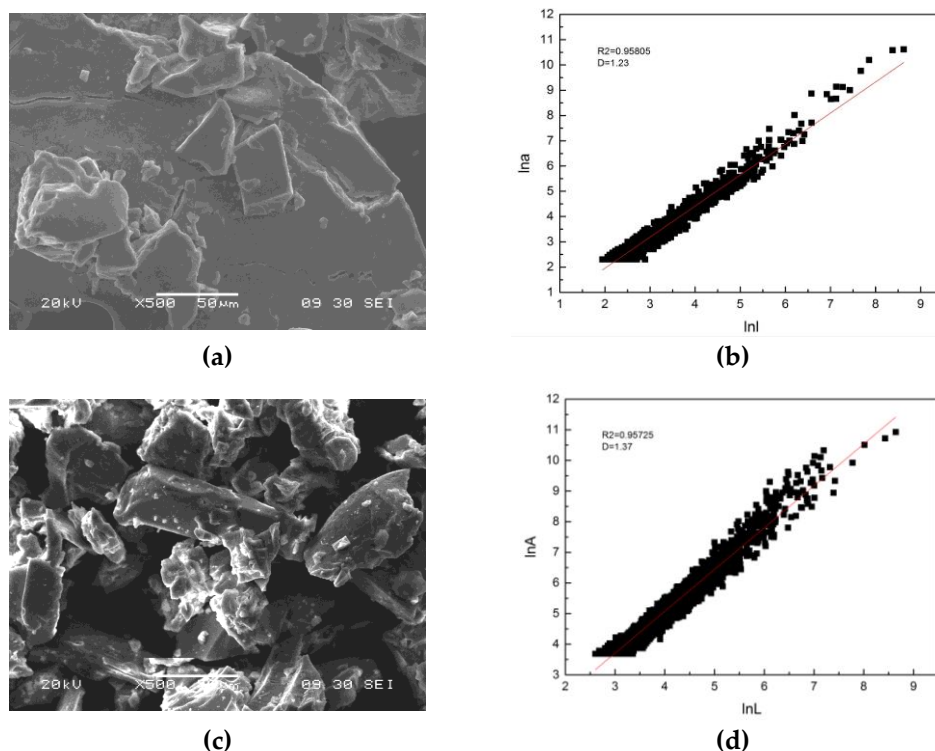


Figure 12. The XRD pattern of polyaluminum chloride (PAC).

### 3.2.3. Scanning Electron Microscopy and Energy Spectrum Analysis

SEM images were obtained and are shown in Figure 13 to investigate the amorphous morphology and intuitively observe the surface visualized information of copolymers. (a) is the electron micrographs of PAC obtained by amplification of 500 times, and (c) is the electron micrographs of PATC obtained by amplification of 500 times. Figure 13b,d show that the fractal dimensions of PAC and PATC were analyzed by Image-Pro Plus 6.0 (Maryland, USA).



**Figure 13.** The SEM of PATC and PAC: (a) Electron micrographs of PAC obtained by amplification of 500 times; (b) Fractal dimensions of PAC; (c) Electron micrographs of PATC obtained by amplification of 500 times; (d) Fractal dimensions of PATC.

The peripheral area method was adopted as the analysis method. By determining the perimeter and area of the particles, the fractal dimension of the flocculant and the correlation coefficient of the circumference area fitting were determined. The figures indicate that when the linear correlation coefficient of PAC was 0.95805, its fractal dimension was  $D = 1.23$ ; when the linear correlation coefficient of PATC was 0.95725, its fractal dimension was  $D = 1.37$ . As presented in Figure 13, PATC showed an irregular structure, and folded areas appeared on the surface. Furthermore, compared with PAC, the clusters of PATC were more compact and comprised more pores. A potential explanation is that the addition of Ti by the hydrolysis of the complex form of the polymer resulted in the tight structure of PATC. By contrast, the surface of PAC was relatively smooth, and its particle distribution was relatively dispersed. Furthermore, PATC showed a certain network structure possibly because of the introduction of Si in the PATC that increased the molecular chain and molecular weight [34,35]. The large polymer produced by the hydrolysis of Ti and Al and the product of hydrolysis induced the condensation polymerization of the hydroxyl bridge [36,37]. Thus, the ability of sweep flocculation was fully evident in the process of coagulation, thereby, greatly improving the coagulation effect and reducing the coagulation time.

Figure 14 shows the energy spectrum analysis of PAC and PATC. O, Cl, Ti, S, Na, Si, and other elements were observed in PATC. Unlike the result in Figure 14a, it can be found that Ti, Si, and

other elements in PATC that were not found in the polymerization of aluminum chloride. Ti, Si, and polymerized aluminum chloride reacted together to obtain the polymerization product of PATC.

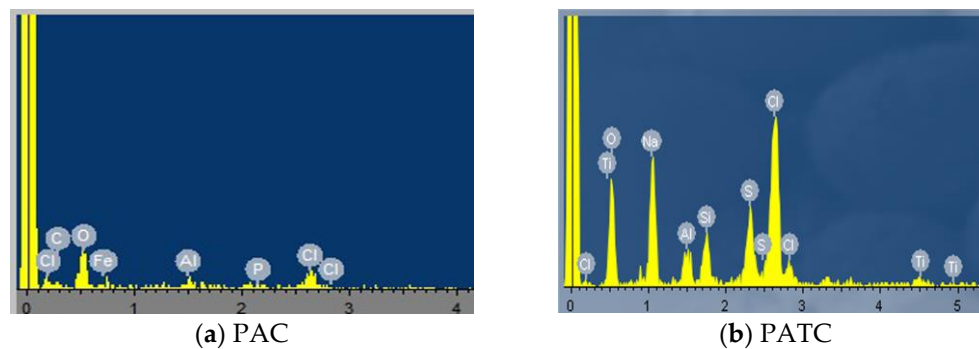
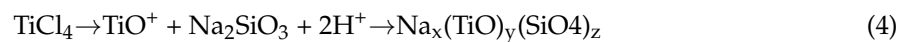
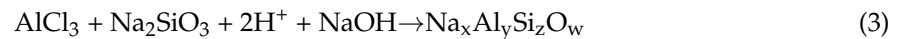
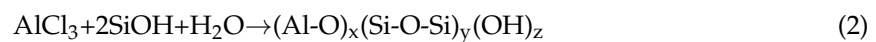


Figure 14. The energy spectrum analysis (EDS) of PAC and PATC.

A possible reaction scheme or mechanism for the formation of PATC from its reagents (Sodium Silicate,  $\text{AlCl}_3$ ,  $\text{TiCl}_4$ ,  $\text{NaOH}$ ) was suggested through the characterization results of PATC and the characteristics of  $\text{TiCl}_4$  hydrolysis and sodium silicate polymerization. The hydrolysis of  $\text{TiCl}_4$  is  $\text{TiCl}_4 \rightarrow \text{H}_2[\text{Ti}(\text{OH})_2\text{Cl}_4] \rightarrow [\text{Ti}(\text{OH})_n(\text{H}_2\text{O})_{6-n}]^{(4-n)+} \rightarrow [\text{Ti}_n(\text{OH})_{2n}(\text{H}_2\text{O})_{2n}]^{2n+} \rightarrow (\text{TiO}_{4n})^{4n-} \rightarrow \text{TiO}_2 \cdot n\text{H}_2\text{O}$ , and the polymerization of sodium silicate is  $\text{Na}_2\text{SiO}_3 + 2\text{H}^+ \rightarrow \text{H}_2\text{SiO}_3 + 2\text{Na}^+$ ,  $2\text{SiOH} \rightarrow \text{SiOSi} + \text{H}_2\text{O}$ ,  $\text{SiOH} + \text{SiO}^- \rightarrow \text{SiOSi} + \text{OH}^-$  [17,38,39]. A possible reaction mechanism for the formation of PATC is:



### 3.3. Flocculation Properties

#### 3.3.1. Orthogonal Experiment

Preliminary experimental research indicated that the coagulant of PATC prepared by this study was effective on low-temperature and low-turbidity water. The initial conditions of the simulated water samples of the orthogonal test included a water temperature of 5 °C. The concentration of humic acid was 10 mg/L, and the pH range was controlled at 5–9. The treatment range of turbidity was 5–25 NTU. The initial turbidity of the water samples was simulated by using a pre-configured kaolin solution. The pH of the simulated water sample was adjusted by using 0.1 mol/L NaOH and 0.1 mol/L HCl. Based on the five factors and five levels identified in Table 1, 25 orthogonal experiments were designed and carried out. The test results are shown in Table 3.

Variance analysis uses the ratio of variance squared sum and error squared sum of each factor as the empirical distribution F function test to determine whether the factors play a significant role.

The significance of factors was determined by the statistic F value and significance level  $p$  value. When  $p < 0.05$ , there was a significant correlation, and the smaller the value, the better the correlation of factors. In this study, the data analysis of the orthogonal experiment was conducted with Minitab software. The  $p = 0.000$  of factor B in Table 4 shows that the amount of coagulant dosage had a significant effect on coagulation. The factor of pH was 0.011 ( $0.01 < 0.011 < 0.05$ ), thereby showing that the pH of the coagulation effect had a significant impact. By contrast, the initial turbidity, stirring intensity, and flocculation settling time did not exert a significant effect on coagulation. It can be determined the effects of these five factors on the treatment of low-turbidity water according to the

size of the  $p$  value in the variance analysis table  $B > C > A > D > E$ . The dosage of PATC and the pH of the simulated water greatly affected the coagulation process.

**Table 3.** Visual analysis of orthogonal test  $L_{25}(5^5)$  using PATC as flocculants.

No.	A	B	C	D	E	Removal Rate of Turbidity (%)
1	1	1	1	1	1	5.395
2	1	2	2	2	2	80.89
3	1	3	3	3	3	87.43
4	1	4	4	4	4	90.46
5	1	5	5	5	5	87.62
6	2	1	2	3	4	35.05
7	2	2	3	4	5	95.05
8	2	3	4	5	1	94.71
9	2	4	5	1	2	88.04
10	2	5	1	2	3	86.6
11	3	1	3	5	2	25.0
12	3	2	4	1	3	91.32
13	3	3	5	2	4	94.87
14	3	4	1	3	5	84.32
15	3	5	2	4	1	92.87
16	4	1	4	2	5	47.83
17	4	2	5	3	1	95.62
18	4	3	1	4	2	66.62
19	4	4	2	5	3	94.95
20	4	5	3	1	4	90.19
21	5	1	5	4	3	24.31
22	5	2	1	5	4	29.46
23	5	3	2	1	5	76.13
24	5	4	3	2	1	91.86
25	5	5	4	3	2	93.36

**Table 4.** Analysis of variance of the orthogonal experiment.

Source	DOF	Seq SS	Adj SS	Adj MS	F	$p$
A Initial turbidity	4	1036.78	1036.78	259.2	6.32	0.051
B the dosage of PATC	4	13,967.12	13,967.12	3491.78	85.2	0.000
C pH	4	2539.59	2539.59	634.9	15.49	0.011
D stirring intensity	4	702.85	702.85	175.71	4.29	0.094
E precipitation time	4	383.75	383.75	95.94	2.34	0.215
Deviation	4	163.94	163.94	40.98		
total	24	18,794.04				

$S = 6.40192$   $R-Sq = 99.13\%$   $R-Sq (adjust) = 94.77\%$ .

Figure 15 shows the main effect diagram of the turbidity removal rate obtained by using the Minitab software. The graph shows that the optimal reaction conditions of PATC for low-turbidity water were A2B5C4D2E5. The optimal reaction conditions were an initial turbidity of 10 NTU, PATC dosage of 9 mg/L, pH of 8 for the simulated water sample, stirring speed of 50 r/min, and settling time of 50 min.

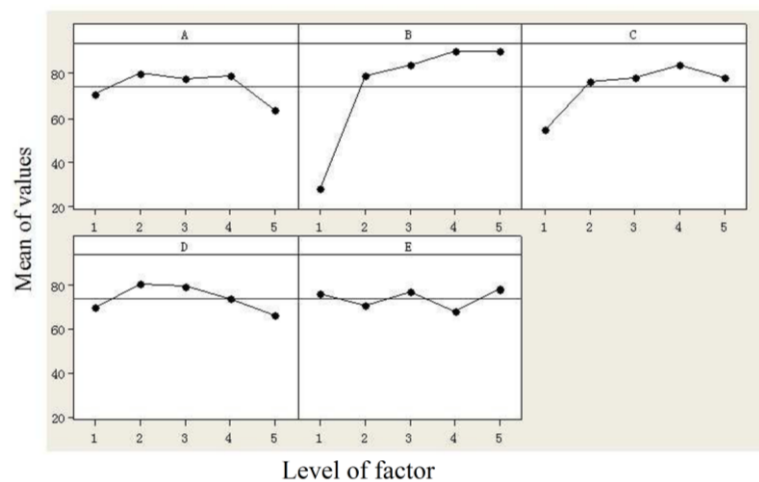


**Figure 15.** The main effect analysis diagram of turbidity removal rate.

### 3.3.2. Potentiometric Analysis

To further explore the mechanism of the reaction between PATC and low-turbidity water under the optimum synthesis conditions of PATC. Thus, in this study, the zeta potential was analyzed for the prepared PATC, the simulated water sample, the flocculant, and the simulated water sample reaction. The results showed that the zeta potential of the coagulant preparation was 2.28 mv and that of the simulated water sample was approximately  $-33$  mv. Figure 16 shows the analysis of the zeta potential of the simulated water under different pH conditions and different dosages. The figure indicates that the zeta potential increased with the addition of PATC into the simulated water sample. Thus, an effect of electrical neutralization occurred, but when the pH was 5 or 6 and the dosage of PATC was 9 mg/L, the zeta potential measured after the flocculant reaction with the simulated water sample remained negative. When the pH was 7, 8, or 9 and the dosage of PATC was 9 mg/L, the zeta potential decreased. Thus, electrical neutralization plays a role in the PATC treatment that simulates the reaction of low-turbidity water. However, the entire flocculation process cannot be completed by electric neutralization alone. The main effects of adsorbing the bridging bridge and sweep flocculation during the flocculation process make the coagulation achieve the best treatment effect. By comparing the simulated water samples with different pH values, it was found that the zeta potential in the reaction became increasingly negative with an increase of pH when the dosage was 1.8 mg/L. A possible reason for this result is that the higher the pH in the more negative charges, the smaller the zeta potential. Given the increased dosage of PATC, the zeta potential increased gradually. Compared with the simulated water samples at pH 5 and 6, those at pH of 7, 8, or 9 and a PATC dosage of 5.4 mg/L showed zeta potentials changing from negative to positive because the pH change caused a change of the degree of hydrolysis of Al and Ti, and further affected the zeta potential change.

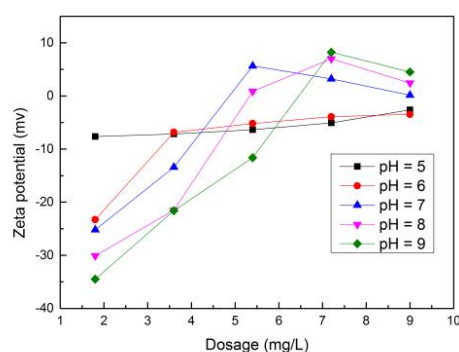


**Figure 16.** Zeta potential of the kaolin-HA with PATC at pH = 5, pH = 6, pH = 7, pH = 8, and pH = 9.



### 3.4. Flocculant Effect Comparison

Table 5 shows the comparison of treatment effects of different aluminium salt and ferric salt flocculants on low turbid water. Additionally, the data of PATC and polyaluminum chloride (PAC) on the treatment effect of low turbid water were obtained from experiments, and water with an initial turbidity of 10 NTU was treated with different dosage of PATC and polyaluminum chloride. The results showed that the treatment effect of PATC on low turbidity water was better than that of polyaluminum chloride, the initial turbidity of 10.3 NTU can be reduced to 0.43 NTU (less than 1 NTU) when the dosage of PATC is 7.2 mg/L, and its removal rate was 95.8%. However, the best treatment of polyaluminum chloride to low turbid water can only reduce turbidity to 1.37 NTU. Moreover, it can be seen from the comparison in Table 5 that the treatment effect of PATC has obvious advantages over that of polysilicic acid, aluminium, and ferric salt (PAFS) and polymerized aluminium ferrum chloride (PAFC) in the treatment of low turbid water, and the minimum turbidity of 0.43 NTU for PATC is comparable to that of the poly-aluminum-titanium-silicate-sulfate (PATS) prepared by Chang et al. (0.36 NTU).

**Table 5.** Comparison of treatment effects of different coagulants on low turbid water.

Coagulants	Dosage	Removal Efficiency	Reference
PATC	3.6 mg/L	19.12%	/
	5.4 mg/L	92.10%	/
	7.2 mg/L	95.80% (10.30 NTU–0.43 NTU)	/
	9.0 mg/L	93.16%	/
PAC	3.6 mg/L	11.40%	/
	5.4 mg/L	87.38% (10.90 NTU–1.37 NTU)	/
	7.2 mg/L	86.70%	/
	9.0 mg/L	–36.8% (Turbidity is higher than original)	/
PATS	0.1 mmol/L	98.10% (19.00 NTU–0.36 NTU)	[3]
PAFC	15.0 mg/L	76.6% (2.05 NTU–0.48 NTU)	[40]
PAFS	16.0 $\mu$ mol/L	86.43 (23.80 NTU–3.23 NTU)	[41]

## 4. Conclusions

PATC was prepared by aluminum chloride, titanium tetrachloride, and sodium silicate. The optimum conditions for preparing PATC were examined, including a reaction temperature of 50 °C,  $n(\text{Ti})/n(\text{Al}) = 0.3$ ,  $n(-\text{OH})/n(\text{Ti}+\text{Al}) = 0.2$ , and  $n(\text{Si})/n(\text{Ti}+\text{Al}) = 1.0$ . The PATC treatment effect on low-turbidity water was superior, with the initial turbidity dropping to 0.53 NTU from 20.75 NTU. The difference in the reaction temperature and raw material ratio directly affected the morphological distribution of Al, thereby resulting in a different treatment effect. Additionally, the analysis of PATC by FTIR and XRD showed that a complex chemical reaction between silicon, aluminum, and titanium in PATC occurred, not just the physical addition. The Ti-O-Si and Si-O-Al bonds formed by the reaction are beneficial to the treatment of low-turbidity water. The SEM analysis showed that, compared with PAC, the clusters of PATC were more compact, and PATC presented a reticular structure that improves the ability of sweep flocculation in coagulation. The coagulation effect was greatly improved, and the coagulation time was shortened.

The optimum conditions for PATC to treat low-turbidity water were determined by an orthogonal test table of five factors and five levels. The optimal reaction conditions were an initial turbidity of 10 NTU, PATC dosage of 9 mg/L, pH of 8 for the simulated water sample, stirring speed of 50 r/min, and settling time of 50 min. The order of influence of these five factors is as follows: Dosage of PATC > pH of simulated water > initial turbidity > stirring intensity > precipitation time. The zeta potential in the process of the reaction was analyzed, and the results show that the reaction process between the flocculant PATC and the low-turbidity water is mainly the function of adsorbing the bridging bridge and sweep flocculation. Electric neutralization plays an auxiliary role, and the simulation of the water pH affects electric neutralization further, thereby influencing the flocculant treatment effect.

**Author Contributions:** P.Z. conceived and designed the experiments; L.L. performed the experiments; P.Z., L.L. analyzed the data; P.Z. contributed reagents/materials/analysis tools.

**Funding:** The authors gratefully acknowledge the support from National Natural Science Foundation of China (Project No. 41502331) and the National Natural Science Foundation of Hunan Province (Project No. 2018JJ3174).

**Conflicts of Interest:** The authors declare no conflict of interest.

## References

1. Razali, M.; Kim, J.F.; Attfield, M.; Budd, P.M.; Drioli, E.; Lee, Y.M.; Szekely, G. Sustainable wastewater treatment and recycling in membrane manufacturing. *Green Chem.* **2015**, *17*, 5196–5205. [[CrossRef](#)]
2. Teixeira, M.R.; Camacho, F.P.; Sousa, V.S.; Bergamasco, R. Green technologies for cyanobacteria and natural organic matter water treatment using natural based products. *J. Clean. Prod.* **2017**, *162*, 484–490. [[CrossRef](#)]
3. Chang, D.W.; Ren, Z.; Wu, W.J. Preparation and characterization of PATS and its effect of coagulation and control of residual aluminum on low-turbidity water treatment. *Chin. J. Environ. Eng.* **2017**, *11*, 4615–4620.
4. Nidheesh, P.V.; Thomas, P.; Nair, K.A.; Joju, J.; Aswathy, P.; Jinisha, R.; Varghese, G.K.; Gandhimathi, R. Potential Use of Hibiscus Rosa-Sinensis Leaf Extract for the Destabilization of Turbid Water. *Water Air Soil Pollut.* **2017**, *228*, 51. [[CrossRef](#)]
5. Folkard, G.K.; Al-Khalili, R.; Sutherland, J.P. *Contact Flocculation Filtration Using a Natural Polyelectrolyte for the Treatment of Low Turbidity Surface Water in Developing Countries*; Springer: Berlin, Germany, 1996; pp. 213–223.
6. Malley, J.P.; Edzwald, J.K. Laboratory Comparison of DAF with Conventional Treatment. *J. Am. Water Works Ass.* **1991**, *83*, 56–61. [[CrossRef](#)]
7. Liang, P.; Ni, Z.H.; Wu, T.; Yao, J.L.; Du, G.L. Research and application of low-temperature and low-turbid water treatment technology. *Water Wastewater Eng.* **2012**, *38*, 76–79.
8. Cheng, W.; Zheng, H.L.; Zhai, J.; Zhao, C.; Xue, W.W.; Cai, N.; Yang, Q.; Li, F. Study on the Preparation of a New Composite Coagulant: Poly-Ferric-Titanium-Sulfate and Analysis of FTIR Spectrum and UV-Vis Spectrum. *Spectrosc. Spect. Anal.* **2016**, *36*, 1038–1043.
9. Shen, Y.H. Treatment of low turbidity water by sweep coagulation using bentonite. *J. Chem. Technol. Biotechnol.* **2005**, *80*, 581–586. [[CrossRef](#)]
10. Xu, W.Y.; Gao, B.Y.; Wang, Y.; Zhang, Q.; Yue, Q.Y. Influences of polysilicic acid in Al 13 species on floc properties and membrane fouling in coagulation/ultrafiltration hybrid process. *Chem. Eng. J.* **2012**, *181*, 407–415. [[CrossRef](#)]
11. Gao, B.Y.; Yue, Q.Y.; Wang, B.J.; Chu, Y.B. Poly-aluminum-silicate-chloride (PASiC)—A new type of composite inorganic polymer coagulant. *Colloid Surf. A* **2003**, *229*, 121–127. [[CrossRef](#)]
12. Dong, H.Y.; Gao, B.Y.; Yue, Q.Y.; Sun, S.L.; Wang, Y.; Li, Q. Floc properties and membrane fouling of polyferric silicate chloride and polyferric chloride: The role of polysilicic acid. *Environ. Sci. Pollut. Res.* **2015**, *22*, 1–9. [[CrossRef](#)] [[PubMed](#)]
13. Moussas, P.A.; Zouboulis, A.I. A study on the properties and coagulation behaviour of modified inorganic polymeric coagulant-Polyferric silicate sulphate (PFSiS). *Sep. Purif. Technol.* **2008**, *63*, 475–483. [[CrossRef](#)]
14. Yang, Z.L.; Gao, B.Y.; Yue, Q.Y. Coagulation performance and residual aluminum speciation of Al<sub>2</sub>(SO<sub>4</sub>)<sub>3</sub> and polyaluminum chloride (PAC) in Yellow River water treatment. *Chem. Eng. J.* **2010**, *165*, 122–132. [[CrossRef](#)]
15. Gázquez, M.J.; Bolívar, J.P.; Garciatenorio, R.; Vaca, F. A review of the production cycle of titanium dioxide pigment. *Mater. Sci. Appl.* **2014**, *5*, 441–458. [[CrossRef](#)]
16. Soriano-Disla, J.M.; Janik, L.; Mclaughlin, M.J.; Forrester, S.; Kirby, J.K.; Reimann, C. Prediction of the concentration of chemical elements extracted by aqua regia in agricultural and grazing european soils using diffuse reflectance mid-infrared spectroscopy. *Appl. Geochem.* **2013**, *39*, 33–42. [[CrossRef](#)]
17. Zhao, Y.X.; Phuntsho, S.; Gao, B.Y.; Huang, X.; Qi, Q.B.; Yue, Q.Y.; Wang, Y.; Kim, J.H.; Shon, H.K. Preparation and Characterization of Novel Polytitanium Tetrachloride Coagulant for Water Purification. *Environ. Sci. Technol.* **2013**, *47*, 12966–12975. [[CrossRef](#)] [[PubMed](#)]
18. Huang, X.; Gao, B.; Yue, Q.Y.; Wang, Y.; Li, Q. Effect of Si/Ti molar ratio on enhanced coagulation performance, floc properties and sludge reuse of a novel hybrid coagulant: Polysilicate titanium sulfate. *Desalination* **2014**, *352*, 150–157. [[CrossRef](#)]

19. Wu, Y.F.; Liu, W.; Gao, N.Y.; Tao, T. A study of titanium sulfate flocculation for water treatment. *Water Res.* **2011**, *45*, 3704–3711. [[CrossRef](#)] [[PubMed](#)]
20. Zhao, Y.X.; Gao, B.Y.; Shon, H.K.; Cao, B.C.; Kim, J.H. Coagulation characteristics of titanium (Ti) salt coagulant compared with aluminum (Al) and iron (Fe) salts. *J. Hazard. Mater.* **2011**, *185*, 1536–1542. [[CrossRef](#)] [[PubMed](#)]
21. Chekli, L.; Galloux, J.; Zhao, Y.X.; Gao, B.Y.; Shon, H.K. Coagulation performance and floc characteristics of polytitanium tetrachloride (PTC) compared with titanium tetrachloride (TiCl<sub>4</sub>) and iron salts in humic acid-kaolin synthetic water treatment. *Sep. Purif. Technol.* **2015**, *142*, 155–161. [[CrossRef](#)]
22. Feng, C.; Shi, B.; Wang, D.; Li, G.; Tang, H. Characteristics of simplified ferron colorimetric solution and its application in hydroxy-aluminum speciation. *Colloid Surf. A* **2006**, *287*, 203–211. [[CrossRef](#)]
23. Deng, B.L.; Luo, H.J.; Jiang, Z.Q.; Jiang, Z.J.; Liu, M.L. Co-polymerization of polysilicic-zirconium with enhanced coagulation properties for water purification. *Sep. Purif. Technol.* **2018**, *200*, 59–67. [[CrossRef](#)]
24. Wunderlich, W.; Vishista, K.; Gnanam, F.D.; Jayaseelan, D.D. Thermodynamical Calculations and Experimental Confirmation about the Mg-Al-Spinel Reaction Path in the Sol-Gel-Process. *Key Eng. Mater.* **2006**, *317*, 135–138. [[CrossRef](#)]
25. Kim, W.B.; Choi, S.H.; Lee, J.S. Quantitative Analysis of Ti-O-Si and Ti-O-Ti Bonds in Ti-Si Binary Oxides by the Linear Combination of XANES. *J. Phys. Chem. B* **2001**, *104*, 8670–8678. [[CrossRef](#)]
26. Okour, Y.; Shon, H.K.; El, S.I. Characterisation of titanium tetrachloride and titanium sulfate flocculation in wastewater treatment. *Water Sci. Technol.* **2009**, *59*, 2463–2473. [[CrossRef](#)] [[PubMed](#)]
27. Yang, Z.L.; Gao, B.Y.; Xu, W.Y.; Cao, B.C.; Yue, Q.Y. Effect of OH<sup>-</sup>/Al<sup>3+</sup> and Si/Al molar ratios on the coagulation performance and residual Al speciation during surface water treatment with poly-aluminum-silicate-chloride (PASiC). *J. Hazard. Mater.* **2011**, *189*, 203–210. [[CrossRef](#)] [[PubMed](#)]
28. Tang, X.M.; Zheng, H.L.; Wang, Y.L.; Chen, W.; Guo, J.S.; Zhou, Y.H.; Li, X. Effect of fresh aluminum hydroxide gels on algae removal from micro-polluted water by polyaluminum chloride coagulant. *J. Taiwan Inst. Chem. E.* **2016**, *63*, 195–201. [[CrossRef](#)]
29. Li, X.; Li, W.; Duan, J.M. Preparation of polysilicate-titanium and its performance as coagulant aid. *Chin. J. Environ. Eng.* **2015**, *9*, 2207–2212.
30. Gao, B.Y.; Yue, Q.Y.; Wang, Z.S.; Tang, H.X. The Coagulating Property of Polyaluminum Silicate Chloride (PASC). *Chin. J. Environ. Sci.* **2000**, *21*, 46–49.
31. Huang, X.; Gao, B.Y.; Wang, Y.; Yue, Q.Y.; Li, Q.; Zhang, Y.Y. Coagulation performance and flocs properties of a new composite coagulant: Polytitanium-silicate-sulfate. *Chem. Eng. J.* **2004**, *245*, 173–179. [[CrossRef](#)]
32. Wang, J.L.; Raza, A.; Si, Y.; Cui, L.X.; Ge, J.F.; Ding, B.; Yu, J.Y. Synthesis of superamphiphobic breathable membranes utilizing SiO<sub>2</sub> nanoparticles decorated fluorinated polyurethane nanofibers. *Nanoscale* **2012**, *4*, 7549–7556. [[CrossRef](#)] [[PubMed](#)]
33. Hayashi, K.; Takahashi, M.; Nomiya, K. Novel Ti-O-Ti bonding species constructed in a metal-oxide cluster. *Dalton Trans.* **2005**, *24*, 3751–3756. [[CrossRef](#)]
34. Zhu, G.C.; Liu, J.F.; Zhou, T.Z.; Zhang, P.; Ren, B.Z.; Zheng, H.L.; Liu, Y.S.; Li, X.M. The Preparation and Characterization of a New Solid Coagulant: Polymeric Ferric Silicate Sulfate. *Spectrosc. Spect. Anal.* **2016**, *36*, 2455–2461.
35. Fu, Y.; Yu, S.L. Characterization and coagulation performance of solid poly-silicic- ferric (PSF) coagulant. *J. Non-Cryst. Solids* **2007**, *353*, 2206–2213. [[CrossRef](#)]
36. Zhao, B.X.; Bai, W.L.; Liang, W.; Zhang, X.L. Study on preparation of polymerized silicate containing zinc sulfate and aluminum sulfate to and its performance. *Chin. J. Environ. Eng.* **2009**, *3*, 2237–2240.
37. Chen, W.; Zheng, H.L.; Zhai, J.; Wang, Y.L.; Xue, W.W.; Tang, X.M.; Zhang, Z.G.; Sun, Y.J. Characterization and coagulation-flocculation performance of a composite coagulant: Poly-ferric-aluminum-silicate-sulfate. *Desalin. Water Treat.* **2015**, *56*, 1776–1786. [[CrossRef](#)]
38. Baillon, F.; Provost, E.; Fürst, W. Study of titanium(IV) speciation in sulphuric acid solutions by FT-Raman spectrometry. *J. Mol. Liq.* **2008**, *143*, 8–12. [[CrossRef](#)]
39. Lange, K.R.; Spencer, R.W. Mechanism of activated silica sol formation. *Environ. Sci. Technol.* **1968**, *2*, 212–216. [[CrossRef](#)]

40. Ma, F.; Meng, L.; Pang, C.L.; Jin, C.; Yao, J. Pilot scale treatment of low turbidity water using compound bioflocculant and polymerized aluminium ferrum chloride. *J. Harbin Inst. Technol. (New Series)* **2009**, *16*, 441–444.
41. Yang, H.Y.; Cui, F.Y.; Zhao, Q.L.; Ma, C. Study on coagulation property of metal-polysilicate coagulants in low turbidity water treatment. *J. Zhejiang Univ. Sci. B* **2004**, *5*, 721–726. [[CrossRef](#)]



© 2018 by the authors. Licensee MDPI, Basel, Switzerland. This article is an open access article distributed under the terms and conditions of the Creative Commons Attribution (CC BY) license (<http://creativecommons.org/licenses/by/4.0/>).